

MARTA BRZEZIŃSKA

BEYOND THE TEN-FOLD WAY: NOVEL TOPOLOGICAL
PHASES IN LOW-DIMENSIONAL SYSTEMS

BEYOND THE TEN-FOLD WAY: NOVEL
TOPOLOGICAL PHASES IN
LOW-DIMENSIONAL SYSTEMS

A dissertation submitted to attain the degree of
DOCTOR OF SCIENCES of WROCŁAW
UNIVERSITY OF SCIENCE AND TECHNOLOGY

presented by
MARTA BRZEZIŃSKA
Master of Science in Physics,
Wrocław University of Science
and Technology, Poland
born on 22 August 1991

supervised by
Prof. Titus Neupert,
Prof. Arkadiusz Wójs,
Dr. Paweł Potasz

2020

ABSTRACT

This thesis covers selected recent developments in the field of topological aspects of condensed matter physics. In particular, we focus on three directions which can be seen as extensions of well-established classification of free-fermionic gapped states: i) investigating a realization of topological states in the systems defined in non-integer spatial dimensions, ii) the role of crystal symmetries and how they affect the distinction between topologically trivial and non-trivial states, and iii) non-Hermitian Hamiltonians arising from a minimal modelling of gains and losses exhibiting observable phenomena without Hermitian counterparts. In all cases, we propose material candidates or experimental setups to support our theoretical findings.

ABSTRAKT

Przedłożona rozprawa doktorska obejmuje wybrane najnowsze osiągnięcia w dziedzinie topologicznych aspektów fizyki materii skondensowanej. W szczególności uwaga zostanie poświęcona trzem kierunkom badań, które można postrzegać jako rozszerzenie ugruntowanej klasyfikacji układów nieoddziałujących fermionów: i) próba realizacji stanów topologicznych w układach scharakteryzowanych przez liczbę wymiarów przestrzennych będących liczbą niecałkowitą, ii) rola symetrii krystalicznych i ich wpływ na rozróżnienie pomiędzy stanami topologicznymi oraz trywialnymi, a także iii) hamiltonianami niehermitowskimi będącymi efektywnym opisem układów otwartych i wykazującymi obserwowalne zjawiska bez odpowiedników w modelach hermitowskich. We wszystkich omawianych zagadnieniach zostaje przedyskutowana możliwa realizacja eksperymentalna w celu poparcia wyników teoretycznych.

ACKNOWLEDGEMENTS

First of all, I would like to thank my supervisors from Wrocław University of Science and Technology, for helping me during the first years of my PhD studies and encouraging me to work in the field of condensed matter physics.

I would like to thank Titus Neupert for giving me the life-changing opportunity to pursue my research in Switzerland and my colleagues from Condensed Matter Theory Group at University of Zurich - I had a great time with having you around.

I also want to thank my family for their constant support and love.

CONTENTS

1	INTRODUCTION	1
2	TOPOLOGICAL BAND THEORY	5
2.1	Notion of topology	5
2.1.1	Homotopy and equivalence classes	5
2.2	Symmetries and classification of topological insulators and superconductors	5
2.3	Topological invariants	7
2.3.1	Chern number	7
2.3.2	Z_2 topological index	7
2.4	Topical examples	8
2.4.1	Class BDI: Su-Schrieffer-Heeger chain	8
2.4.2	Class A: integer quantum Hall states and Chern insulators	9
2.4.3	Class AII: quantum spin Hall effect	10
3	TOPOLOGICAL STATES IN SELF-SIMILAR LATTICES	11
3.1	Real-space methods for computing topological invariants	11
3.2	Edge states	12
3.3	Effect of disorder	14
4	OBSTRUCTED ATOMIC LIMITS	17
4.1	Crystal symmetries	17
4.2	Wannier representation	17
4.3	Corner charges	18
4.3.1	Charge fractionalization in 1D	18
4.4	Bulk indices	18
4.4.1	Symmetry indicators	18
4.4.2	Wilson loops	19
4.5	Material candidates	19
5	TOPOLOGY IN NON-HERMITIAN SYSTEMS	21
5.1	Exceptional points	22
5.2	Breakdown of bulk-boundary correspondence	22
5.3	Skin effect	23
5.3.1	Reciprocal skin effect	23
6	SUMMARY	25
A	BAND THEORY	27
A.0.1	General definitions	27
A.0.2	Wannier functions	28
A.0.3	Group theory: representations and character table	28

BIBLIOGRAPHY 29

ABBREVIATIONS

1D	one-dimensional
2D	two-dimensional
BZ	Brillouin zone
CB	conduction band
NN	nearest-neighbour
NNN	next-nearest-neighbour
QH	quantum Hall
SOC	spin-orbit coupling
SPT phase	symmetry protected topological phase
TI	topological insulator
VB	valence band

INTRODUCTION

Classification is a theme that lies at the heart of condensed matter physics. For a long time, it was believed that Ginzburg-Landau theory [1] of the phase transitions based on the symmetry-breaking paradigm provides a complete list of phases of matter. It states that the continuous transition between phases is described by a local order parameter, which vanishes in the high-symmetry (disordered) phase and becomes non-zero in the low-symmetry (ordered) phase. For instance, magnetization serves as an order parameter at the ferromagnetic-paramagnetic transition; crystals break continuous translational symmetry and hence are characterized by a discrete space group. Another example is superconductivity, where the non-zero gap Δ indicates the superconducting state.

At the beginning of 1970s, Berezinskii [2, 3], Kosterlitz and Thouless [4, 5] investigated a two-dimensional classical magnet with $U(1)$ (XY model) in which the phase transition falls beyond the Ginzburg-Landau paradigm. At the zero-temperature, the system is ferromagnetic as the spins are perfectly arranged. At finite (but small) temperature, the system still has long-range correlations but a local spin structures called vortices may be created. Vortices are said to be topological excitations as the only way to destroy them is to annihilate vortex with an antivortex. With an increase of the temperature, more pairs of vortex-antivortex pairs are created and they become less bounded, hence destroying the long-range correlations. This is the Kosterlitz-Thouless (KT) phase transition in which no continuous symmetry is spontaneously broken (which is in an agreement with Mermin-Wagner theorem), yet the system undergoes a transition to the phase with short-range correlations. For their developments in the field of topological matter, Kosterlitz and Thouless (together with Haldane) obtained the Nobel Prize in 2016.

An even more pronounced example is a discovery of the integer quantum Hall effect (IQHE) [6], and subsequently, the fractional version of this phenomenon (FQHE) [7]. In a two-dimensional electron gas at low temperature exposed to a strong magnetic field, applying the voltage on the two sides of a sample results in a current generated in the perpendicular direction. As a function of the magnetic field, one observes the perfectly flat plateaus in the transverse Hall conductivity, while the longitudinal conductivity vanishes. Hall conductivity σ_{xy} takes quantized values being multiplies ν (ν is an integer in case of IQHE, while a fraction in case of

FQHE) of elementary constants e^2/h (where e is the electron charge and h is the Planck constant) and has been measured to the accuracy of the order 10^{-9} [8]. For the discovery of IQHE, Klaus von Klitzing got the Nobel Prize in 1985 and now the quantum of conductance serves as a universal constant. The origin of this quantization is universal, in a sense that it is observed regardless of microscopic details of a sample such as disorder. In a finite geometry, the systems exhibits robust edge currents, which are chiral, that is they flow in one fixed direction. These are two different manifestations of the topological properties of the systems.

IQH states can be understood from the perspective of the Landau levels formed in a strong magnetic field. A remarkable idea given by Thouless, Kohmoto, Nightingale, and den Nijs (TKNN) [9] was to relate the number of gapless edge modes with the topological invariant computed for the bulk. This became the first observation of the *bulk-boundary correspondence*. Later on, the theoretical proposals of realization of IQH states on the honeycomb lattice in the absence of magnetic field [10] or topological superconductors [11] ignited the experimental search for topological materials. On the other hand, understanding FQHE requires taking into account the electron-electron interactions. The exotic properties emerge from the collective behavior of electrons and give rise to the concept of topological order as the low-energy effective theory can be described in terms of topological quantum field theories (such as Chern-Simons or BF). Apart from FQHE, another paradigmatic example of topological order is chiral spin liquid developed as an attempt to understand high-temperature superconductivity [12, 13]. Topologically ordered states may posses unique features such as fractionalized excitations (carrying the fractions of elemental charge) with the anyonic exchange statistic (not bosonic nor fermionic) or long-range entanglement pattern [14]. In addition, they exhibit robust ground state degeneracy depending on the manifold on which they are defined. These properties are very promising for a fault-tolerant quantum computing [15].

As no symmetry breaking occurs, in order to classify topological phases a notion of equivalence classes has to be introduced. To do so, we will investigate the systems at zero temperature with a spectral gap separating the ground state from the first excited state. States are said to be topologically equivalent if they can be connected by unitary transformations that act infinitely slowly (adiabatically). The physical constrains of unitaries are that at every point of evolution they have to preserve the energy gap and they have to involve only local degrees of freedom. In addition, one may take into account the symmetries to enlarge the number of possible unitary transformations and investigate symmetry-protected (or symmetry-enriched) topological states.

Not all the states that are topological possess intrinsic topological order: some of them may be short-range entangled and they can be understood from the single-particle physics perspective (a more detailed explanation will be given in the following chapter). Interestingly, a lot of theoretical developments were followed-up by experimental efforts.

ORGANIZATION OF THIS THESIS

In this thesis, we study non-interacting fermionic systems which cannot be completely classified by means of the so-called ten-fold way, that is the classification based on a dimensionality and the presence or absence of internal symmetries: time-reversal, particle-hole and chiral.

Chapter 2 serves as a brief introduction to topological band theory, with an emphasis on the basic definitions, topological invariants and illustrative examples of toy models.

In Chapter 3, a realization of topological states in systems with non-integer spatial dimension is discussed. Detecting topological properties without the translational invariants requires employing real-space methods.

Chapter 4 is devoted to the states protected by the crystalline symmetries. However, they fall beyond a sharp distinction what is topological or trivial. Obstructed atomic limits are recent refinements and can be understood from the perspective of Wannier functions.

Topological states in non-Hermitian systems are investigated in Chapter 5. Recently, a studies of non-Hermitian Hamiltonians emerged as an effective modeling of open systems in which the energy or particle number is not preserved.

Finally, Chapter 6 provides a summary and indicates further directions. In addition, some lengthy derivations are given in Appendix ??.

TOPOLOGICAL BAND THEORY

In this chapter, we introduce more formally the concept of topology in the band theory. We provide the definitions of topological invariants, precise the bulk-boundary correspondence, and discuss the details of the classification for gapped free-fermion models.

2.1 NOTION OF TOPOLOGY

Topology is a branch of mathematics that deals with properties of smooth, continuous transformations. We briefly introduce fundamental concepts [Nakahara].



FIGURE 2.1: From a perspective of topology, the

2.1.1 Homotopy and equivalence classes

Hence, in order to change

2.2 SYMMETRIES AND CLASSIFICATION OF TOPOLOGICAL INSULATORS AND SUPERCONDUCTORS

In quantum mechanics, the symmetries are constructed according to the Wigner's theorem: they are the operators that preserve transition probabilities and are therefore implemented via unitaries or antiunitaries which commute with the Hamiltonian.

A local unitary symmetry can be decomposed as $U = U_1 \dots U_n$, where each U_i affects only a small region in space. Conversely, a non-local unitary

A fundamental example of antiunitary operator is the time-reversal, which takes $t \rightarrow -t$. Acting on Hamiltonian H :

$$\mathcal{T}H\mathcal{T}^{-1} = +H \quad (2.1)$$

		\mathcal{T}	\mathcal{P}	\mathcal{C}	$d = 1$	$d = 2$	$d = 3$
standard	A (unitary)	0	0	0	-	\mathbb{Z}	-
	AI (orthogonal)	+1	0	0	-	-	-
	AII (symplectic)	-1	0	0	-	\mathbb{Z}_2	\mathbb{Z}_2
chiral	AIII (chiral unitary)	0	0	1	\mathbb{Z}	-	\mathbb{Z}
	BDI (chiral orthogonal)	+1	+1	1	\mathbb{Z}	-	-
	CII (chiral symplectic)	-1	-1	1	\mathbb{Z}	-	\mathbb{Z}_2
BdG	D	0	+1	0	\mathbb{Z}_2	\mathbb{Z}	-
	C	0	-1	0	-	\mathbb{Z}	-
	DIII	-1	+1	1	\mathbb{Z}_2	\mathbb{Z}_2	\mathbb{Z}
	CI	+1	-1	1	-	-	\mathbb{Z}

TABLE 2.1: Table of symmetry classes of non-interacting Hamiltonians taken from Refs. [17] and [18]

As all antiunitary operators, \mathcal{T} can be decomposed into a product of a unitary operator T and complex conjugate \mathcal{K} , $\mathcal{T} = T\mathcal{K}$. Applying \mathcal{T} twice will lead to the rise of the phase factor, hence $\mathcal{T}^2 = \pm 1$. This is true for all antiunitary symmetries. For spin-1/2 systems, TRS systems follow the Kramers' theorem which tells that all states comes in time-reversal symmetric pairs $\mathcal{T}|n\rangle = |n\rangle$.

Another (antiunitary) symmetry is the particle-hole \mathcal{P} , defined as:

$$\mathcal{P}H\mathcal{P}^{-1} = -H \quad (2.2)$$

Finally, we can define chiral symmetry being a product of \mathcal{T} and \mathcal{P} , $\mathcal{C} = \mathcal{T}\mathcal{P}$ ¹

$$\mathcal{C}H\mathcal{C}^{-1} = -H \quad (2.3)$$

\mathcal{C} may be present in the system, even if \mathcal{T} and \mathcal{P} are absent. Although chiral symmetry is not a symmetry in a strict sense, but guarantees that non-zero eigenvalues of the Hamiltonian come in pairs, hence there is a spectral symmetry.

Dates back to the idea of Élie Cartan's classification of symmetric spaces in differential geometry. Later on, Altland and Zirnbauer applied this classification in the context of random matrix theory [16]

All possible combination of internal symmetries in $d = 1, 2, 3$ spatial dimensions are tabulated in Tab. 2.1. There are ten distinguished classes.

¹ Note that \mathcal{P} and \mathcal{C} anticommute with the single-particle Hamiltonian

This was first proposed in Ref. [19], with further mathematical improvements from K-theory (such is pattern called Bott periodicity; with a period two for the complex classes AI, AIII and a period eight for remaining eight real classes) given by Kitavev [18] to finally provide the complete classification [17].

For higher dimensions, topological invariants repeat themselves and show the Bott periodicity with period 2 for classes A and AIII, and period 8 for the remaining ones.

2.3 TOPOLOGICAL INVARIANTS

Berry connection of Bloch states:

$$\mathbf{A} = i \langle u_n(\mathbf{k}) | \Delta | u_m(\mathbf{k}) \rangle \quad (2.4)$$

$\Delta \equiv \Delta_{\mathbf{k}}$ Berry curvature:

$$F = \Delta \times \mathbf{A} \quad (2.5)$$

Gauss-Bonnet theorem for a two-dimensional manifold M without a boundary:

$$\int_M K dA = 2\pi(2 - 2g) \quad (2.6)$$

with K being the Gauss curvature and g - genus.

2.3.1 Chern number

For two-dimensions, it is given by the (first) Chern number:

$$C = \frac{1}{2\pi} \int_{BZ} F \quad (2.7)$$

(note, some conventions incorporate imaginary unit i explicitly in the prefactor).

2.3.2 Z_2 topological index

Some systems can have one trivial and one topological phase, which is characterized by a two-valued index ν being 0 or 1, respectively. Z_2 invariant can be computed easily in the presence of inversion symmetry using Fu-Kane formula [20]:

$$\delta_i = \prod_{m=1}^N \xi_{2m}(\Gamma_i); \quad (-1)^\nu = \prod_i \delta_i \quad (2.8)$$

where Γ_i are time-reversal invariant momenta in the BZ, $\xi_{2m}(\Gamma_i)$ is every second occupied Kramers pair. In case of 3D systems, two types of TI can be observed, defined whether they have a strong or weak indices. Non-zero strong index means that the system cannot be seen as a set of stacked 2D layers, it's intrinsically three-dimensional.

Because for TRS systems C always vanishes, if S_z (spin component pointing out of 2D plane) is conserved, one may define the spin Chern number [21] based on the fact that spins up and down have independent Chern numbers:

$$C_s = \frac{C_{\uparrow} - C_{\downarrow}}{2} \quad (2.9)$$

and is related to ν as $\nu = C_s \bmod 2$

Pfaffian formalism

2.4 TOPICAL EXAMPLES

In the following, we would like to discuss relevant examples of toy models and discuss experimental realizations.

2.4.1 Class BDI: Su-Schrieffer-Heeger chain

SSH model, firstly proposed to describe polyacetylene, describes spinless fermions in 1D chain [22]

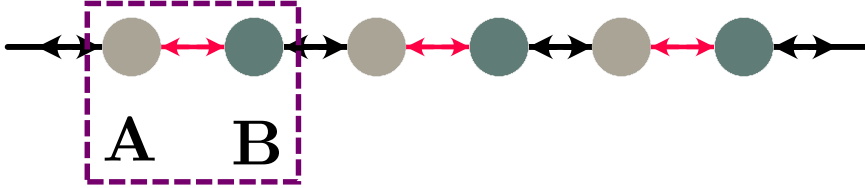


FIGURE 2.2: A schematic of SSH chain. There are two atomic sites A and B per unit cell and alternating hoppings with strength t (within unit cell) and t' (between neighbouring unit cells). Depending on t and t' , the model exhibits two phases: if $t' > t$, the system is in a topological phase with gapless edge modes in an open geometry; conversely, if $t' < t$ the system is in a trivial phase with $t' = 0$ as a fully dimerized case.

Bloch Hamiltonian reads:

$$H(k) = \begin{pmatrix} 0 & t + t'e^{ik} \\ t + t'e^{-ik} & 0 \end{pmatrix} \quad (2.10)$$

Dispersion

$$E(k) = \pm \sqrt{t^2 + t'^2 + 2tt' \cos k} \quad (2.11)$$

The system has the chiral symmetry realized by σ_z , particle-hole $P = \sigma_z \mathcal{K}$ and time-reversal $\mathcal{T} = \mathcal{K}$. Here, It is the chiral symmetry that protects the topological properties and, for instance, adding long range hoppings would destroy topological states.

2.4.2 Class A: integer quantum Hall states and Chern insulators

IQH states can be seen as the most robust topological states without intrinsic topological order as they don't need any symmetry to persist. In particular, TR is broken. Actually, in the classification based on the entanglement (Wen vs. Kitaev)

Haldane model is a first example of a Chern insulator, where TR symmetry is broken because of complex NNN hopping. Experimental realizations include fermionic ultracold atoms [23] or classical wave systems [24].

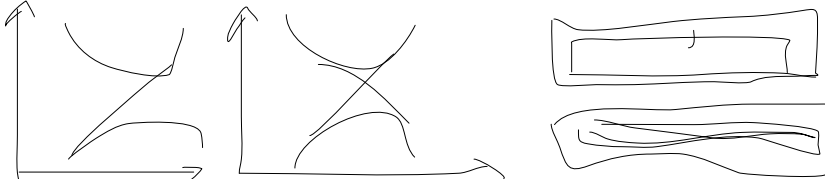


FIGURE 2.3: Left: Schematic representation of the band structures of (a) Chern insulator with $C = +1$ and (b) QSH system constructed as two copies of CI with opposite Chern numbers, together with conserved z-spin component. Right: Edge modes flowing in samples

2.4.3 Class AII: quantum spin Hall effect

In 2005, Kane and Mele extended the notion of Chern insulators by taking two copies of Haldane model with opposite chiralities [25]. This led to the construction of an insulating state which is time-reversal invariant and has protected gapless edge modes lying in the bulk gap, where the topological properties are defined by a \mathbb{Z}_2 invariant. Edge states are helical - that is, they are two states counterpropagate along a boundary. They also come in time-reversal pairs according to the Kramers' theorem. States with odd number of Kramers' edge pairs are topological, while with even number - are topologically trivial. Another consequence of the TR symmetry is that energy levels crossing appear only at special points in the BZ. Authors suggested that this model may be realized in graphene, however due to negligible spin-orbit coupling, it is not realizable experimentally under realistic conditions [26, 27]. Besides fundamental theoretical interest, QSH states hold great promise for spintronics as it is possible to manipulate spin degrees of freedom in the absence of magnetic field [28].

Subsequently, QSH effect was proposed in strained zinc-blende semiconductors (such as gallium arsenide) [29]. Bernevig, Hughes and Zhang [30] predicted a quantum phase transition in HgTe/CdTe quantum wells as a function of the thickness. This happens because of a band inversion due to strong spin-orbit coupling in HgTe: CB has a p -like character and VB is composed of s -orbitals instead of normal ordering which is observed in CdTe: s -orbital character of conduction band and p -orbital of valence band. It was confirmed experimentally year later by observing quantized resistance $h^2/2e$ (factor 2 comes from the spin contribution) [31]. This ignited a search for new materials exhibiting QSH states [32, 33], and topological insulators in three-dimensions.

In Ref. [34]

TOPOLOGICAL STATES IN SELF-SIMILAR LATTICES

Underlying geometry in quantum lattice models plays an important role in their electronic properties. For instance, frustration in spin models on triangular or kagome lattices arises due to inability of defining unique ground state which minimizes the total energy.

Having a

Interestingly, the authors in pointed out that topological states can be realized in amorphous lattice models [35]. BHZ on fractals [36]

Experimental realizations: CO molecules on a Cu (111) surface [37], assembled molecules [38], focused ion beam epitaxy [39], in metamaterials that mimic the physics of quantum models (amorphous Chern insulators [40]).

Prediction of peculiar transport properties: [41, 42]

3.1 REAL-SPACE METHODS FOR COMPUTING TOPOLOGICAL INVARIANTS

Disordered or amorphous systems, due to lack of translational invariance, require defining topological invariants in a real space. Insights from non-commutative geometry have provided to be useful. Here, we discuss the real-space invariants for the relevant symmetry class A.

Bott index

To use the Bott index, which measures the commutativity of the projected position operators. Algorithm for computing the Bott index [43].

$$\begin{aligned} U &= P e^{i2\pi X} P \\ V &= P e^{i2\pi Y} P \end{aligned} \tag{3.1}$$

where X, Y are the coordinates, rescale to fit the interval $[0, 1)$.

$$B = \frac{1}{2\pi} \text{Im} \left(\text{Tr} [\log(VUV^\dagger U^\dagger)] \right) \tag{3.2}$$

which requires to take a logarithm of a matrix.

Chern number

$$\mathcal{C} = 12\pi i \sum_{j \in A} \sum_{k \in B} \sum_{l \in C} \left(P_{jk} P_{kl} P_{lj} - P_{jl} P_{lk} P_{kj} \right), \quad (3.3)$$

where P is the projector operator onto occupied states and i, j, l label the lattice sites.

Fractal lattices comprise of many interesting features: they are aperiodic, but scale invariant. Also, there is no sharp notion between bulk and edge.

Here, we are interested in the lattice regularization of two fractals, Sierpiński carpet (SC) and triangle (or gasket) (SG). This approach is relevant for potential experimental realization as it introduces the distance between nearest-neighbouring sites (lattice constant) to be a natural cutoff.

The reason why we investigate these lattices is motivated by their distinct Hausdorff dimensions ($d_H = \ln A / \ln L$, where A is the area and L the linear size) and connectivity properties. Firstly, $d_H = 1.892 \dots$ for SC and $d_H = 1.585 \dots$ for SG.

We consider tight-binding model of spinless electrons exposed to a magnetic field. The Hamiltonian reads

$$H = -t \sum_{\langle i,j \rangle} e^{iA_{ij}} c_i^\dagger c_j + \text{h.c.}, \quad (3.4)$$

where we set $t = 1$. Introducing a finite field leads to lifting the macroscopic degeneracy

In Fig. 3.1 we observe Hofstadter's butterfly [44]

One of the difficulties is to compute topological invariants in that systems as they do not exhibit translational invariance. One may therefore employ real-space methods. Other methods (for example, the Bott index) may be numerically insufficient. Here, we used the real-space expression for the Chern number:

To compute the Chern number as a function of the Fermi level, we use the formula Eq. (3.3).

3.2 EDGE STATES

Edge-locality marker:

$$\mathcal{B}_{\lambda,l} = \sum_{i \in \mathcal{E}_l} |\psi_{\lambda,i}|^2, \quad (3.5)$$

Previous studies for fractal lattices [45, 46] suggested that the presence of a magnetic field leads to an increase in the degree of delocalization

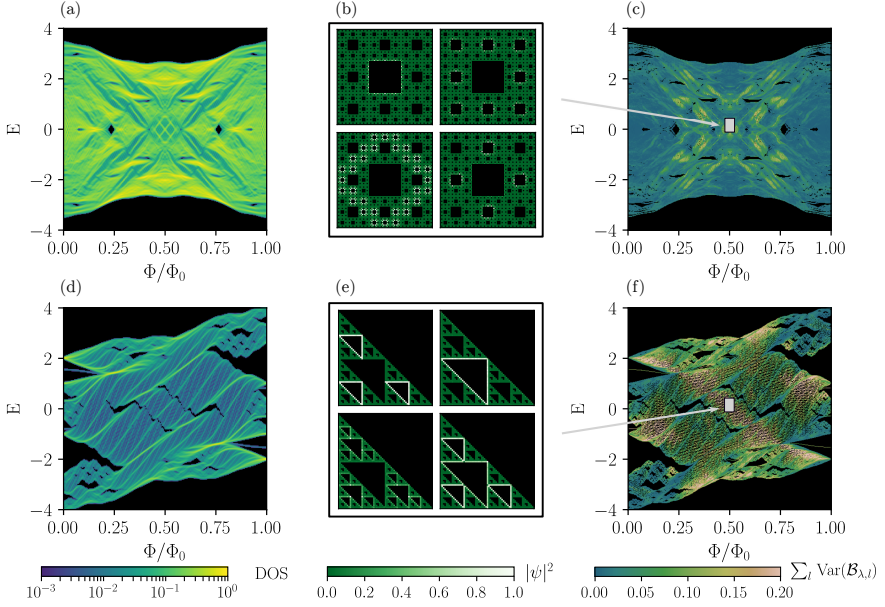


FIGURE 3.1: Density of states, localization of selected eigenstates and edge-locality marker.

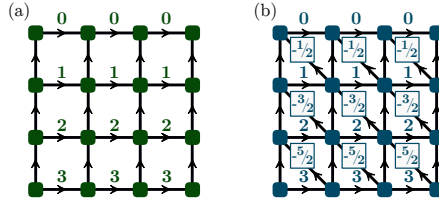


FIGURE 3.2: Phase distribution on 4×4 (a) square and (b) triangle lattices with open boundary conditions. A_{ij} phase between site i and j is equal to the number shown above the bond in 2π units. A phase acquired with the respect to the direction pointed by arrows has a positive sign.

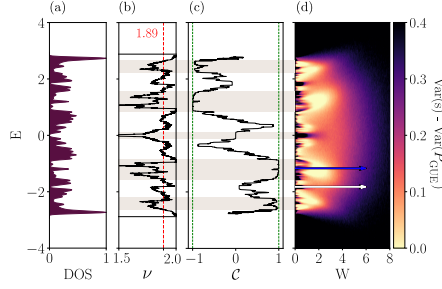


FIGURE 3.3: Density of states at $\Phi/\Phi_0 = 1/4$, scaling of density of states, the Chern number and disorder-induced phase transition.

of eigenstates. This can be confirmed by calculating inverse participation ratio:

$$I_\psi = \frac{\sum_i |\psi_i|^4}{(\sum_i |\psi_i|^2)^2}. \quad (3.6)$$

At zero flux $\alpha = 0$, i.e., in absence of a magnetic field, the distribution of IPRs is peaked close to the inverse of the number of sites belonging to the edges of the second-smallest squares or triangles. As magnetic field is introduced, exemplified here with $\alpha = 0.02$, the distribution of IPRs shifts to smaller, i.e., more delocalized values. This effect is more pronounced for the SC compared to the SG.

3.3 EFFECT OF DISORDER

As an ultimate probe, we study potential topological phase transition with the level spacing statistics. Depending whether states are extended or localized, they follow Wigner-Dyson or Poisson distribution, respectively. Such approach was successfully applied to disordered topological and Chern insulators [47, 48]

However, authors in Ref. [49] claim that a power-law like level statistics is a generic feature of fractals.

To do so, we add the on-site disorder term $\sum_i V_i c_i^\dagger c_i$ in Eq. (3.4), where V_i is drawn from a uniform distribution $[-W/2, W/2]$. Having computed the level spacings, we calculate their variance and average over 500 disorder realizations for each disorder strength W .

It is worth mention that follow-up works investigated the Hall conductance in Sierpiński carpet. It was found that the edge states corresponding to non-zero σ_{xy} are always present for a finite field strength and stable as one approaches the thermodynamic limit [50]. Interestingly, the Hall conductivity is not proportional to the Chern number KatnelsonFractal2020.

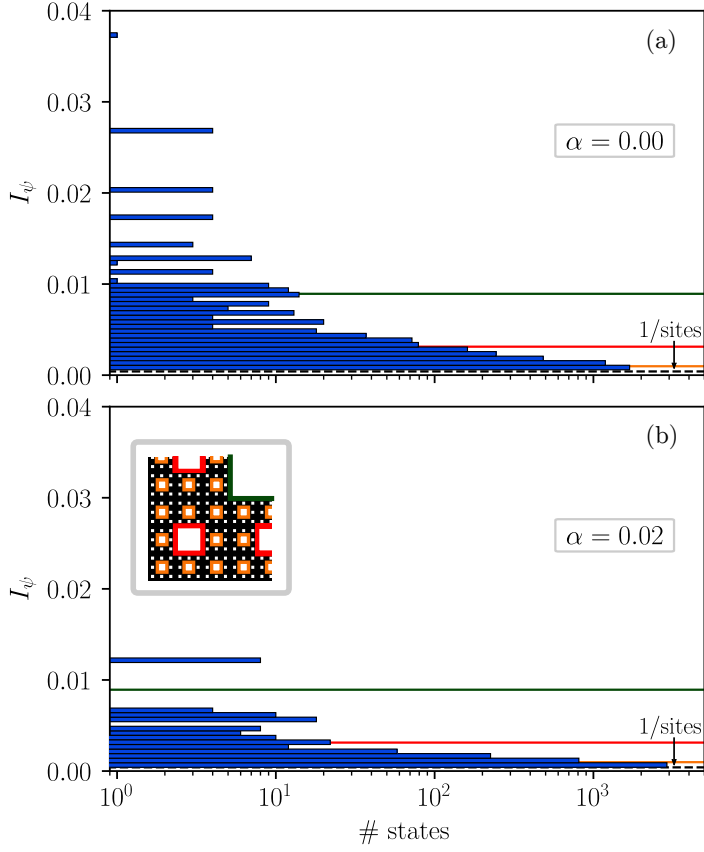


FIGURE 3.4: Distribution of IPR for SC at (a) $\alpha = 0$ and (b) $\alpha = 0.02$. Inset: a closeup of carpet with internal edges of different hierarchies indicated by distinct colors.

Models realizing spinless chiral p - and $p + ip$ -wave superconductors on SC and SG were discussed in [51]

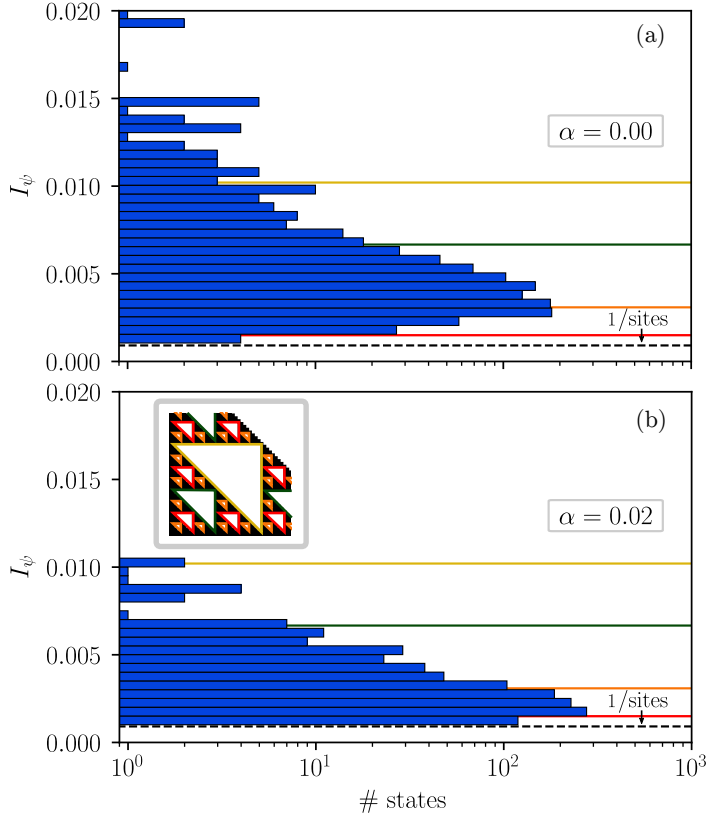


FIGURE 3.5: Statistics of IPR for SG at (a) $\alpha = 0$ and (b) $\alpha = 0.02$. Inset: a closeup of gasket with highlighted edges of different hierarchies.

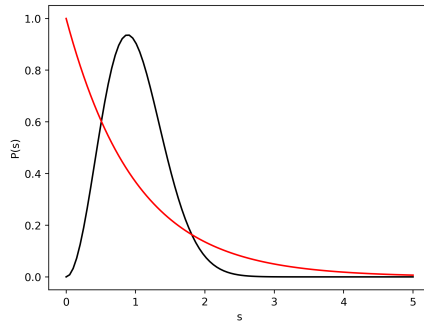


FIGURE 3.6: Comparison of the level spacing distribution

OBSTRUCTED ATOMIC LIMITS

4.1 CRYSTAL SYMMETRIES

In Chapter ??, we discussed the role of **internal** symmetries. Now let us move to the symmetries in crystals (formal definitions are given in Appendix A).

Gapless boundary modes in topological crystalline insulators are protected by spatial symmetries which act non-locally (i.e. mirror symmetry $M_z : x \rightarrow -x$ Prediction of 3D TCI with two-dimensional surface states in the semiconducting SnTe protected by the mirror symmetry [52, 53].

Extending the classification schemes to crystal symmetries [54–58].

Crystal symmetries give rise to a generalization of TIs called higher-order topological insulators, where non-trivial d -dimensional bulk is accompanied by boundary modes in less than $(d - 1)$ -dimensions [59–61]. For instance, 3D system may exhibit 1D hinge modes/

The group of symmetry operations that leave a point, line or plane in momentum space invariant is called its little group

A general framework of topological quantum chemistry [62]

4.2 WANNIER REPRESENTATION

Strong topological phases Recently, an important question has been asked: the fact that there are obstructions to the Wannier representation guarantees stable topology? It turned out that it is not [63]. Actually, the bands may exhibit a **fragile topology** which means that they do not obey Wannier representation, but may be trivialized by adding degrees of freedom.

On the other hand, obstructed atomic limits admit the Wannier function representation, (with Wannier functions being exponentially localized and symmetry-preserving). However, the Wannier centers do not coincide with atomic positions (as in the case of trivial atomic limit), but they are rather localized on other symmetric points in the unit cell called the Wyckoff positions.



FIGURE 4.1: In the presence of crystal symmetries, a distinction between topological and trivial phases is less pronounced. Atomic limit corresponds to the situation where Wannier charge centers are located on atomic positions. In case of obstructed atomic limits, Wannier functions are exponentially localized on the Wyckoff positions. Fragile phases cannot be represented in terms of Wannier functions, but a strong index vanishes. Strong topological phases (such as TI or CI) do not admit Wannier representation.

4.3 CORNER CHARGES

4.3.1 Charge fractionalization in 1D

Detection of fractional charges with entanglement spectrum [64].

Note that the charge fractionalization mechanism is different that in, for example, spin liquids. Here it's due to cutting Wannier functions in a finite sample.

4.4 BULK INDICES

The key goal was to construct the bulk indices for all layer groups to be sure that boundary effects are related to the nontrivial bulk rather than suitable edge termination.

4.4.1 Symmetry indicators

Fu-Kane formula presented in Chapter 2 was actually the first symmetry indicator. In a similar manner, one may construct the quantities which will count

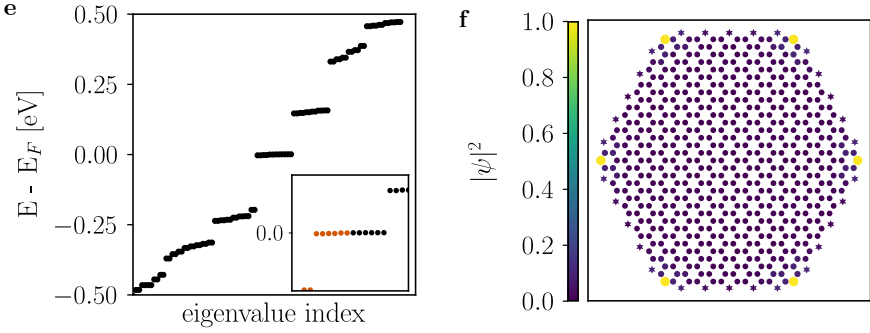


FIGURE 4.2: Low-energy spectrum of a finite armchair-terminated flake of the 3cOAL. The inset presents the energies around the Fermi level, with filled states in orange. (f) The electronic densities of the corner states with color scale proportional to the normalized square modulus of the eigenstates $|\psi|^2$ (normalized with respect to the largest $|\psi|^2$). The tellurium atoms used for edge passivation are shown as stars.

4.4.2 Wilson loops

(Non)-Abelian Wilson loops can be seen as a generalization of the one-dimensional Berry phase. As a unitary matrix, it can be written as

$$W[\gamma] = \exp \left(- \int_{\gamma} \text{Im} m d\mathbf{l} A(\mathbf{k}) \right) \quad (4.1)$$

Given the projector onto occupied states $P := \sum_{E < E_F} |\psi\rangle \langle \psi|$, the Wilson loop is defined as a product of P along closed path γ in k -space:

$$W_{\gamma} = \prod_{\mathbf{k}} P(\mathbf{k}) \quad (4.2)$$

and it is gauge invariant.

4.5 MATERIAL CANDIDATES

Predicted also in atomically thin carbon allotrope called graphdiyne [65, 66].

As potential experimental realization, we propose group-V honeycomb monolayers of bismuth, antimony and arsenic.

A bismuth itself was among first materials predicted to be a QSH insulator [34]

They share the very same crystal structure. With non-zero buckling, these systems preserve C_3 and \bar{C}_2 . When $d_z = 0$, TCI phase is exhibited.

In Fig. 4.2 we show

In quantum mechanics, the condition that the observable must be a Hermitian operator has a deep physical reasoning - the corresponding expectation value has to be a real-valued number. However, this strong assumption can be relaxed - it is possible to have a non-Hermitian operator with real spectrum. This observation gave rise to the concept of PT-symmetric Hamiltonians, where the real spectrum is guaranteed by the product of parity and time-reversal symmetries [67].

Another motivation comes from the open systems. Instead of a full treatment with Lindblad formalism, for instance, nH Hamiltonians can effectively capture the coupling of the system with its environment, where the non-Hermiticity models the gains and losses.

Such system exhibits interesting phenomena without Hermitian counterpart: exceptional points, the skin effect and, as a consequence, the breakdown of bulk-boundary correspondence.

Novel features of nH systems are seen at the level of 2×2 matrices. Consider a matrix M : $M =$

$$\begin{pmatrix} 0 & \alpha \\ 1 & 0 \end{pmatrix} \quad (5.1)$$

If $\alpha \neq 1$, M is not diagonalizable, and only admits the Jordan block form. NH matrices have distinct left- and right- eigenvectors. Therefore, a remedy for some problems may be to consider quantities of interests within the biorthogonal quantum mechanics. For instance, the norm is then given by the inner product between left and right eigenvectors. This attempt allowed to restore BB correspondence in some models. Another way is to consider the singular value decomposition (SVD) instead of eigenvalue problem. However, the interpretation of the singular values is not physical (in contrast to the eigendecomposition, where the eigenvalues are the energies) [68].

In non-Hermitian case, the topology is already manifested in single-band systems (in contrast to Hermitian systems where at least two bands are needed). Also, the winding number for 1D systems is defined through the eigenvalues, not the eigenstates.

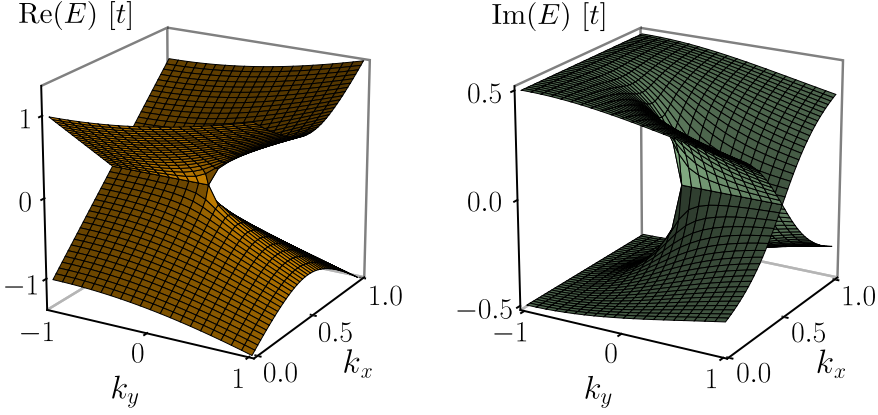


FIGURE 5.1: Real (left) and imaginary (right) part of the spectrum of the Hamiltonian defined by Eq.(5.3). Gapless region of real part of the spectrum corresponds to gapped imaginary spectrum and vice versa.

5.1 EXCEPTIONAL POINTS

Let us remind the concept of Weyl points. Consider the Hamiltonian in 3D

$$H = \mathbf{k} \cdot \boldsymbol{\sigma} = k_x \sigma_x + k_y \sigma_y + k_z \sigma_z. \quad (5.2)$$

This model exhibits a robust generic degeneracy. As all σ_i are used, adding other term proportional to σ_i only shifts the touching point. Now compare the following model in 2D:

$$H = k_x \sigma_x + k_y \sigma_y + ir \sigma_y \quad (5.3)$$

Non-zero r gives rise to the degeneracies in non-Hermitian band structure called exceptional points. Exceptional points can be seen as equivalents of Weyl nodes as they appear in generic points in k -space and one has to get them closer to annihilate them (for example by adding very large mass term).

5.2 BREAKDOWN OF BULK-BOUNDARY CORRESPONDENCE

As Hermitian conjugate is not longer equal to complex conjugate and transpose, different type of symmetries appear. Classification, firstly by [69], extended recently in Refs. [70–72]

5.3 SKIN EFFECT

nH Hamiltonians are sensitive to the boundary conditions. Eigenstates localization properties may change dramatically. All states for the system in an open geometry may be exponentially localized on the one edge, which is dubbed the skin effect (note: this has nothing in common with a typical skin effect, where the electrons in a conductor prefer to flow far from the middle due to electron-electron repulsion).

Previously, it was known that the skin effect can be induced by having unbalanced directed hoppings. However, this breaks the reciprocity, defined as

$$H(k) = H^T(-k) \quad (5.4)$$

5.3.1 *Reciprocal skin effect*

Here, we show that in two- or higher-dimensions it is possible to have the skin effect with the condition defined by Eq. (5.4).

SUMMARY

It is of great interest to provide a systematic classification for the systems with the scale symmetry instead of translational invariance.

BAND THEORY

We recap the formalism for translational invariant lattice models described within the tight-binding approximation for non-interacting particles.

A.0.1 General definitions

This imposes only quadratic terms in creation and annihilation operators in the second-quantized Hamiltonian. We define a crystal as a regular arrangement of the unit cells at positions \mathbf{R}_n

$$\mathbf{R}_n = n_1 \mathbf{a}_1 + n_2 \mathbf{a}_2 + n_3 \mathbf{a}_3, \quad i = 1, 2, 3 \quad \text{and} \quad \mathbf{n} = (n_1, n_2, n_3) \in \mathbb{R}^3 \quad (\text{A.1})$$

where $\{\mathbf{a}_i\}$ are the linearly independent basis vectors. We can define the reciprocal lattice vectors $\{\mathbf{b}_i\}$

$$\mathbf{G}_m = m_1 \mathbf{b}_1 + m_2 \mathbf{b}_2 + m_3 \mathbf{b}_3, \quad m_i \in \mathbb{Z} \quad (\text{A.2})$$

satisfying

$$\mathbf{a}_i \cdot \mathbf{a}_j = 2\pi \delta_{ij}, \quad i, j = 1, 2, 3 \quad (\text{A.3})$$

constructed

$$\mathbf{b}_i = 2\pi \frac{\mathbf{a}_j \times \mathbf{a}_k}{\mathbf{a}_i \cdot (\mathbf{a}_j \times \mathbf{a}_k)} \quad \text{and} \quad \mathbf{a}_i = 2\pi \frac{\mathbf{b}_j \times \mathbf{b}_k}{\mathbf{b}_i \cdot (\mathbf{b}_j \times \mathbf{b}_k)} \quad (\text{A.4})$$

$$\mathbf{R}_n \cdot \mathbf{G}_m = 2\pi (n_1 m_1 + n_2 m_2 + n_3 m_3) = 2\pi N, \quad (\text{A.5})$$

with N being an integer.

Brillouin zone is the unit cell of the reciprocal lattice.

The Bloch's theorem states that the Schrodinger equation for translationally invariant Hamiltonians can be solved by a wave function $\psi = e^{ikt}u$ where u is the periodic part of the Bloch function and identical in every unit cell.

A.0.2 Wannier functions

Another basis for the single-particle Hilbert spaces can be constructed using Wannier states. Given a set of occupied Bloch states, one may construct the Wannier function as their Fourier transform:

$$|\mathbf{R}, n\rangle = \frac{V}{(2\pi)^3} \int_{\text{BZ}} d\mathbf{k} e^{i\mathbf{k}\cdot\mathbf{R}} \sum_{m=1}^J U_{mn}(\mathbf{k}) |\psi_{m\mathbf{k}}\rangle. \quad (\text{A.6})$$

Wannier functions are not uniquely defined - there is a gauge freedom. For instance, multiplying the Bloch state by $U(1)$ phase factor $\phi(\mathbf{k})$; $|\mathbf{k}, n\rangle \rightarrow e^{i\phi(\mathbf{k})} |\mathbf{k}, n\rangle$, which acts locally in reciprocal space, leaves the physical observables invariant. However, it changes the shape of basis functions in real space, only the sum over the Wannier centers in a given unit cell remains the same. Most often, the rotation matrix U_{nm} is determined in such a way the minimizes the spread in real space (= the sum of the mean squares) of the Wannier function. For more detailed discussion, we refer to the review by Marziari *et al.* [73].

A.0.3 Group theory: representations and character table

Here, we recall basic notions from group theory [74]. A group \mathbb{G} has the properties:

- the product of two elements of \mathbb{G} is also in \mathbb{G} : $a, b \in \mathbb{G} \Rightarrow a \star b = c \in \mathbb{G}$
- there is a unit element $e \in \mathbb{G}$ that satisfies $e \star a = a \star e = a, \forall a \in \mathbb{G}$
- multiplication is associative: $a \star (b \star c) = (a \star b) \star c$
- for every element $a \in \mathbb{G}$, there is an inverse $a^{-1} \in \mathbb{G} \Rightarrow a^{-1} \star a = a \star a^{-1} = e$.

A group is call Abelian if for all elements $a \star b = b \star a$, otherwise it is non-Abelian.

A representation of a group over some vector space V is a collection of linear operators on this vector space, which satisfy the same algebra as the group elements. For finite groups, these operators can be simply matrices. Then, an irreducible representation is a set of matrix operators that are block-diagonalized simultaneously and cannot be divided into smaller parts.

BIBLIOGRAPHY

1. Ginzburg, V. L. & Landau, L. D. On the Theory of superconductivity. *Zh. Eksp. Teor. Fiz.* **20**, 1064 (1950).
2. Berezinsky, V. L. Destruction of long range order in one-dimensional and two-dimensional systems having a continuous symmetry group. I. Classical systems. *Sov. Phys. JETP* **32**. [*Zh. Eksp. Teor. Fiz.*59,907(1971)], 493 (1971).
3. Berezinsky, V. L. Destruction of Long-range Order in One-dimensional and Two-dimensional Systems Possessing a Continuous Symmetry Group. II. Quantum Systems. *Sov. Phys. JETP* **34**. [*Zh. Eksp. Teor. Fiz.*61,no.3,1144(1972)], 610 (1972).
4. Kosterlitz, J. M. & Thouless, D. J. Long range order and metastability in two dimensional solids and superfluids. (Application of dislocation theory). *Journal of Physics C: Solid State Physics* **5**, L124 (1972).
5. Kosterlitz, J. M. & Thouless, D. J. Ordering, metastability and phase transitions in two-dimensional systems. *Journal of Physics C: Solid State Physics* **6**, 1181 (1973).
6. Klitzing, K. v., Dorda, G. & Pepper, M. New Method for High-Accuracy Determination of the Fine-Structure Constant Based on Quantized Hall Resistance. *Phys. Rev. Lett.* **45**, 494 (6 1980).
7. Tsui, D. C., Stormer, H. L. & Gossard, A. C. Two-Dimensional Magnetotransport in the Extreme Quantum Limit. *Phys. Rev. Lett.* **48**, 1559 (22 1982).
8. Mohr, P. J., Newell, D. B. & Taylor, B. N. CODATA Recommended Values of the Fundamental Physical Constants: 2014. *Journal of Physical and Chemical Reference Data* **45**, 043102 (2016).
9. Thouless, D. J., Kohmoto, M., Nightingale, M. P. & den Nijs, M. Quantized Hall Conductance in a Two-Dimensional Periodic Potential. *Phys. Rev. Lett.* **49**, 405 (6 1982).
10. Haldane, F. D. M. Model for a Quantum Hall Effect without Landau Levels: Condensed-Matter Realization of the "Parity Anomaly". *Phys. Rev. Lett.* **61**, 2015 (18 1988).
11. Read, N. & Green, D. Paired states of fermions in two dimensions with breaking of parity and time-reversal symmetries and the fractional quantum Hall effect. *Phys. Rev. B* **61**, 10267 (15 2000).

12. Wen, X. G. Vacuum degeneracy of chiral spin states in compactified space. *Phys. Rev. B* **40**, 7387 (10 1989).
13. Wen, X. G., Wilczek, F. & Zee, A. Chiral spin states and superconductivity. *Phys. Rev. B* **39**, 11413 (16 1989).
14. Wen, X.-G. Colloquium: Zoo of quantum-topological phases of matter. *Rev. Mod. Phys.* **89**, 041004 (4 2017).
15. Nayak, C., Simon, S. H., Stern, A., Freedman, M. & Das Sarma, S. Non-Abelian anyons and topological quantum computation. *Rev. Mod. Phys.* **80**, 1083 (3 2008).
16. Altland, A. & Zirnbauer, M. R. Nonstandard symmetry classes in mesoscopic normal-superconducting hybrid structures. *Phys. Rev. B* **55**, 1142 (2 1997).
17. Ryu, S., Schnyder, A. P., Furusaki, A. & Ludwig, A. W. W. Topological insulators and superconductors: tenfold way and dimensional hierarchy. *New Journal of Physics* **12**, 065010 (2010).
18. Kitaev, A. Periodic table for topological insulators and superconductors. *AIP Conference Proceedings* **1134**, 22 (2009).
19. Schnyder, A. P., Ryu, S., Furusaki, A. & Ludwig, A. W. W. Classification of topological insulators and superconductors in three spatial dimensions. *Phys. Rev. B* **78**, 195125 (19 2008).
20. Fu, L. & Kane, C. L. Topological insulators with inversion symmetry. *Phys. Rev. B* **76**, 045302 (4 2007).
21. Sheng, D. N., Weng, Z. Y., Sheng, L. & Haldane, F. D. M. Quantum Spin-Hall Effect and Topologically Invariant Chern Numbers. *Phys. Rev. Lett.* **97**, 036808 (3 2006).
22. Su, W. P., Schrieffer, J. R. & Heeger, A. J. Solitons in Polyacetylene. *Phys. Rev. Lett.* **42**, 1698 (25 1979).
23. Jotzu, G., Messer, M., Desbuquois, R., Lebrat, M., Uehlinger, T., Greif, D. & Esslinger, T. Experimental realization of the topological Haldane model with ultracold fermions. *Nature* **515**, 237 (2014).
24. Ding, Y., Peng, Y., Zhu, Y., Fan, X., Yang, J., Liang, B., Zhu, X., Wan, X. & Cheng, J. Experimental Demonstration of Acoustic Chern Insulators. *Phys. Rev. Lett.* **122**, 014302 (1 2019).
25. Kane, C. L. & Mele, E. J. Quantum Spin Hall Effect in Graphene. *Phys. Rev. Lett.* **95**, 226801 (22 2005).
26. Min, H., Hill, J. E., Sinitsyn, N. A., Sahu, B. R., Kleinman, L. & MacDonald, A. H. Intrinsic and Rashba spin-orbit interactions in graphene sheets. *Phys. Rev. B* **74**, 165310 (16 2006).

27. Yao, Y., Ye, F., Qi, X.-L., Zhang, S.-C. & Fang, Z. Spin-orbit gap of graphene: First-principles calculations. *Phys. Rev. B* **75**, 041401 (4 2007).
28. Hasan, M. Z. & Kane, C. L. Colloquium: Topological insulators. *Rev. Mod. Phys.* **82**, 3045 (4 2010).
29. Bernevig, B. A. & Zhang, S.-C. Quantum Spin Hall Effect. *Phys. Rev. Lett.* **96**, 106802 (10 2006).
30. Bernevig, B. A., Hughes, T. L. & Zhang, S.-C. Quantum Spin Hall Effect and Topological Phase Transition in HgTe Quantum Wells. *Science* **314**, 1757 (2006).
31. König, M., Wiedmann, S., Brüne, C., Roth, A., Buhmann, H., Molenkamp, L. W., Qi, X.-L. & Zhang, S.-C. Quantum Spin Hall Insulator State in HgTe Quantum Wells. *Science* **318**, 766 (2007).
32. Liu, C., Hughes, T. L., Qi, X.-L., Wang, K. & Zhang, S.-C. Quantum Spin Hall Effect in Inverted Type-II Semiconductors. *Phys. Rev. Lett.* **100**, 236601 (23 2008).
33. Knez, I., Du, R.-R. & Sullivan, G. Evidence for Helical Edge Modes in Inverted InAs/GaSb Quantum Wells. *Phys. Rev. Lett.* **107**, 136603 (13 2011).
34. Murakami, S. Quantum Spin Hall Effect and Enhanced Magnetic Response by Spin-Orbit Coupling. *Phys. Rev. Lett.* **97**, 236805 (23 2006).
35. Agarwala, A. & Shenoy, V. B. Topological Insulators in Amorphous Systems. *Phys. Rev. Lett.* **118**, 236402 (23 2017).
36. Agarwala, A., Pai, S. & Shenoy, V. B. Fractalized Metals. *ArXiv e-prints* (2018).
37. Kempkes, S. N., Slot, M. R., Freney, S. E., Zevenhuizen, S. J. M., Vanmaekelbergh, D., Swart, I. & Smith, C. M. Design and characterization of electrons in a fractal geometry. *Nature Physics* **15**, 127 (2019).
38. Shang, J., Wang, Y., Chen, M., Dai, J., Zhou, X., Kuttner, J., Hilt, G., Shao, X., Gottfried, J. M. & Wu, K. Assembling molecular Sierpinski triangle fractals. *Nature Chemistry* **7**, 389 (2015).
39. Chen, T. L., Dikken, D. J., Prangsma, J. C., Segerink, F. & Herek, J. L. Characterization of Sierpinski carpet optical antenna at visible and near-infrared wavelengths. *New Journal of Physics* **16**, 093024 (2014).
40. Mitchell, N. P., Nash, L. M., Hexner, D., Turner, A. M. & Irvine, W. T. M. Amorphous topological insulators constructed from random point sets. *Nature Physics* **14**, 380 (2018).
41. Van Veen, E., Yuan, S., Katsnelson, M. I., Polini, M. & Tomadin, A. Quantum transport in Sierpinski carpets. *Phys. Rev. B* **93**, 115428 (11 2016).

42. Van Veen, E., Tomadin, A., Polini, M., Katsnelson, M. I. & Yuan, S. Optical conductivity of a quantum electron gas in a Sierpinski carpet. *Phys. Rev. B* **96**, 235438 (23 2017).
43. Loring, T. A. & Hastings, M. B. Disordered topological insulators via C^* -algebras. *EPL (Europhysics Letters)* **92**, 67004 (2010).
44. Hofstadter, D. R. Energy levels and wave functions of Bloch electrons in rational and irrational magnetic fields. *Phys. Rev. B* **14**, 2239 (6 1976).
45. Banavar, J. R., Kadanoff, L. & Pruisken, A. M. M. Energy spectrum for a fractal lattice in a magnetic field. *Phys. Rev. B* **31**, 1388 (3 1985).
46. Wang, X. R. Magnetic-field effects on localization in a fractal lattice. *Phys. Rev. B* **53**, 12035 (18 1996).
47. Prodan, E., Hughes, T. L. & Bernevig, B. A. Entanglement Spectrum of a Disordered Topological Chern Insulator. *Phys. Rev. Lett.* **105**, 115501 (11 2010).
48. Prodan, E. Disordered topological insulators: a non-commutative geometry perspective. *Journal of Physics A: Mathematical and Theoretical* **44**, 113001 (2011).
49. Iliasov, A. A., Katsnelson, M. I. & Yuan, S. Power-law energy level spacing distributions in fractals. *Phys. Rev. B* **99**, 075402 (7 2019).
50. Fremling, M., van Hooft, M., Smith, C. M. & Fritz, L. Existence of robust edge currents in Sierpiński fractals. *Phys. Rev. Research* **2**, 013044 (1 2020).
51. Pai, S. & Prem, A. Topological states on fractal lattices. *Phys. Rev. B* **100**, 155135 (15 2019).
52. Fu, L. Topological Crystalline Insulators. *Phys. Rev. Lett.* **106**, 106802 (10 2011).
53. Hsieh, T. H., Lin, H., Liu, J., Duan, W., Bansil, A. & Fu, L. Topological crystalline insulators in the SnTe material class. *Nature Communications* **3**, 982 (2012).
54. Slager, R.-J., Mesaros, A., Juricic, V. & Zaanen, J. The space group classification of topological band-insulators. *Nature Physics* **9**, 98 (2013).
55. Shiozaki, K. & Sato, M. Topology of crystalline insulators and superconductors. *Phys. Rev. B* **90**, 165114 (16 2014).
56. Shiozaki, K., Sato, M. & Gomi, K. Topology of nonsymmorphic crystalline insulators and superconductors. *Phys. Rev. B* **93**, 195413 (19 2016).
57. Shiozaki, K., Sato, M. & Gomi, K. Topological crystalline materials: General formulation, module structure, and wallpaper groups. *Phys. Rev. B* **95**, 235425 (23 2017).

58. Dong, X.-Y. & Liu, C.-X. Classification of topological crystalline insulators based on representation theory. *Phys. Rev. B* **93**, 045429 (4 2016).
59. Benalcazar, W. A., Bernevig, B. A. & Hughes, T. L. Quantized electric multipole insulators. *Science* **357**, 61 (2017).
60. Langbehn, J., Peng, Y., Trifunovic, L., von Oppen, F. & Brouwer, P. W. Reflection-Symmetric Second-Order Topological Insulators and Superconductors. *Phys. Rev. Lett.* **119**, 246401 (24 2017).
61. Schindler, F., Cook, A. M., Vergniory, M. G., Wang, Z., Parkin, S. S. P., Bernevig, B. A. & Neupert, T. Higher-order topological insulators. *Science Advances* **4** (2018).
62. Bradlyn, B., Elcoro, L., Cano, J., Vergniory, M. G., Wang, Z., Felser, C., Aroyo, M. I. & Bernevig, B. A. Topological quantum chemistry. *Nature* **547**, 298 (2017).
63. Po, H. C., Watanabe, H. & Vishwanath, A. Fragile Topology and Wannier Obstructions. *Phys. Rev. Lett.* **121**, 126402 (12 2018).
64. Zhu, P., Loehr, K. & Hughes, T. L. Identifying C_n -symmetric higher-order topology and fractional corner charge using entanglement spectra. *Phys. Rev. B* **101**, 115140 (11 2020).
65. Sheng, X.-L., Chen, C., Liu, H., Chen, Z., Yu, Z.-M., Zhao, Y. X. & Yang, S. A. Two-Dimensional Second-Order Topological Insulator in Graphdiyne. *Phys. Rev. Lett.* **123**, 256402 (25 2019).
66. Lee, E., Kim, R., Ahn, J. & Yang, B.-J. Two-dimensional higher-order topology in monolayer graphdiyne. *npj Quantum Materials* **5**, 1 (2020).
67. Bender, C. M. & Boettcher, S. Real Spectra in Non-Hermitian Hamiltonians Having PT Symmetry. *Phys. Rev. Lett.* **80**, 5243 (24 1998).
68. Herviou, L., Bardarson, J. H. & Regnault, N. Defining a bulk-edge correspondence for non-Hermitian Hamiltonians via singular-value decomposition. *Phys. Rev. A* **99**, 052118 (5 2019).
69. Bernard, D. & LeClair, A. A Classification of Non-Hermitian Random Matrices. *Statistical Field Theories*, 207 (2002).
70. Shen, H., Zhen, B. & Fu, L. Topological Band Theory for Non-Hermitian Hamiltonians. *Phys. Rev. Lett.* **120**, 146402 (14 2018).
71. Gong, Z., Ashida, Y., Kawabata, K., Takasan, K., Higashikawa, S. & Ueda, M. Topological Phases of Non-Hermitian Systems. *Phys. Rev. X* **8**, 031079 (3 2018).
72. Liu, C.-H., Jiang, H. & Chen, S. Topological classification of non-Hermitian systems with reflection symmetry. *Phys. Rev. B* **99**, 125103 (12 2019).

- 73. Marzari, N., Mostofi, A. A., Yates, J. R., Souza, I. & Vanderbilt, D. Maximally localized Wannier functions: Theory and applications. *Rev. Mod. Phys.* **84**, 1419 (4 2012).
- 74. Dresselhaus, M., Dresselhaus, G. & Jorio, A. *Group Theory: Application to the Physics of Condensed Matter* (Springer Berlin Heidelberg, 2007).

CURRICULUM VITAE

PERSONAL DATA

Name	Marta Agnieszka Brzezińska
Date of Birth	August 22, 1991
Place of Birth	Legnica, Poland

EDUCATION

since 2015	Ph. D. in Physics, Faculty of Fundamental Problems of Technology, Wrocław University of Technology, Poland Supervisors: Prof. Titus Neupert, Prof. Arkadiusz Wójs
2013 – 2015	M. Sc. in Physics, Faculty of Fundamental Problems of Technology, Wrocław University of Technology, Poland Specialization: Physical Foundations of Computer Science Thesis: Entanglement entropy in d-dimensional interacting many-body systems Supervisor: Prof. Arkadiusz Wójs Grade: 5.5 (excellent)
2010 – 2013	B. Sc. in Physics, Faculty of Fundamental Problems of Technology, Wrocław University of Technology, Poland Grade: 5.0 (very good)

SCHOLARSHIPS

Sep 2019 – Aug 2020	The Iwanowska Programme for Doctoral Students from Polish National Agency for Academic Exchange
Sep 2018 – Aug 2019	Swiss Government Excellence Scholarship from Federal Commission for Scholarships for Foreign Students

PUBLICATIONS

Articles in peer-reviewed journals:

1. Schindler, F., Brzezińska, M., Benalcazar, W. A., Iraola, M., Bouhon, A., Tsirkin, S. S., Vergniory, M. G. & Neupert, T. Fractional corner charges in spin-orbit coupled crystals. *Phys. Rev. Research* **1**, 033074 (3 2019).
2. Guguchia, Z., Gawryluk, D. J., Brzezińska, M., Tsirkin, S. S., Khasanov, R., Pomjakushina, E., von Rohr, F. O., Verezhak, J. A. T., Hasan, M. Z., Neupert, T., Luetkens, H. & Amato, A. Nodeless superconductivity and its evolution with pressure in the layered dirac semimetal 2M-WS₂. *npj Quantum Materials* **4**, 50 (2019).
3. Brzezińska, M., Cook, A. M. & Neupert, T. Topology in the Sierpiński-Hofstadter problem. *Phys. Rev. B* **98**, 205116 (20 2018).
4. Nouri, N., Bieniek, M., Brzezińska, M., Modarresi, M., Borujeni, S. Z., Rashedi, G., Wójs, A. & Potasz, P. Topological phases in Bi/Sb planar and buckled honeycomb monolayers. *Physics Letters A* **382**, 2952 (2018).
5. Brzezińska, M., Bieniek, M., Woźniak, T., Potasz, P. & Wójs, A. Entanglement entropy and entanglement spectrum of Bi_{1-x}Sb_x (111) bilayers. *Journal of Physics: Condensed Matter* **30**, 125501 (2018).
6. Radosz, W., Mielnik-Pyszcorski, A., Brzezińska, M. & Sznajd-Weron, K. Q-voter model with nonconformity in freely forming groups: Does the size distribution matter? *Phys. Rev. E* **95**, 062302 (6 2017).

Preprints (available on arXiv):

1. Hofmann, T., Helbig, T., Schindler, F., Salgo, N., Brzezińska, M., Greiter, M., Kiessling, T., Wolf, D., Vollhardt, A., Kabaši, A., Lee, C. H., Bilušić, A., Thomale, R. & Neupert, T. *Reciprocal skin effect and its realization in a topoelectrical circuit* 2019.
2. Potasz, P., Jaworowski, B., Kupczyński, M., Brzezińska, M., Kaczmarkiewicz, P. & Wójs, A. *Topological phase transitions in Chern insulators within three-band models* 2017.